

Distribution Agreement

In presenting this thesis as a partial fulfillment of the requirements for a degree from Emory University, I hereby grant to Emory University and its agents the non-exclusive license to archive, make accessible, and display my thesis in whole or in part in all forms of media, now or hereafter now, including display on the World Wide Web. I understand that I may select some access restrictions as part of the online submission of this thesis. I retain all ownership rights to the copyright of the thesis. I also retain the right to use in future works (such as articles or books) all or part of this thesis.

Suraj Pothineni

April 9, 2018

Pore Size Dependence of Hydrodynamic Friction in Hydrogels on Smooth Surfaces

By

Suraj Pothineni

Justin Clifford Burton
Adviser

Physics Department

Justin Clifford Burton
Adviser

Jed Brody
Committee Member

Douglas Mulford
Committee Member

2019

Pore Size Dependence on Hydrodynamic Friction in Hydrogels on Smooth Surfaces

By

Suraj Pothineni

Justin Clifford Burton

Adviser

An abstract of
a thesis submitted to the Faculty of Emory College of Arts and Sciences
of Emory University in partial fulfillment
of the requirements of the degree of
Bachelor of Arts with Honors

Physics Department

2019

Abstract

Pore Size Dependence on Hydrodynamic Friction in Hydrogels on Smooth Surfaces

By Suraj Pothineni

Hydrogels are three-dimensional polymer matrices capable of absorbing large volumes of water. Because of their features such as biocompatibility, temperature resistance and sensitivity, they are extensively being used in industrial and agricultural applications, ranging from diaper linings that absorb the moisture away from the baby's skin to boosting water retention in soil. Hydrogels' other unique mechanical properties such as a low friction make them promising biomaterials that have potential to be used as prime candidates for biosensors, drug-delivery vectors and improved contact lenses. Their extensive use and quirky qualities drive the need to further our understanding of the mechanical behavior of these hydrogels. Using a custom low-force tribometer, we investigated gel friction of spherical hydrogels on acrylic discs under a variety of environmental conditions. Previous research has indicated that gel frictional coefficients as a function of speed follow a non-monotonic trend. Upon reaching a critical sliding velocity, we observed a dynamic frictional transition with transient behavior. Our results can be interpreted as a competition between the shear rate in the fluid versus the relaxation time it takes the polymer chains to return to equilibrium after being disturbed. Before we establish a set model for this regime, we investigated hydrodynamic frictional behavior for velocities leading up to the critical velocity. Our results showed a pore size dependence on friction of hydrogels on smooth surfaces at this low-velocity regime. Having varied several environmental conditions such as gel structure, load and salinity, we determined a relationship between pore size and gel friction.

Pore Size Dependence of Hydrodynamic Friction in Hydrogels on Smooth Surfaces

By

Suraj Pothineni

Justin Clifford Burton

Adviser

A thesis submitted to the Faculty of Emory College of Arts and Sciences
of Emory University in partial fulfillment
of the requirements of the degree of
Bachelor of Arts with Honors

Physics Department

2019

Acknowledgements

First and foremost, I have to thank my mentors, Justin Burton and Nicholas Cuccia, for introducing me to the study of hydrogels and, in general, to scientific research. As a junior with very little experience in research and the physics of soft matter, they taught me everything I need to know to be able to conduct research in such an interesting field of physics that I did not experience in my undergraduate courses. They have given me many opportunities to go to the next level and were there to help each step of the way. Without their assistance and involvement, this paper would not have existed. I would like to thank you very much and am eager to continue researching with Burton Lab in the upcoming few months.

I would also like to thank my committee, including Jed Brody and Douglas Mulford, for taking time out of their schedule to be of guidance and evaluate my thesis. Dr. Brody was my professor for Advanced Laboratory Techniques in Physics. I have learned a lot about research and about the art of writing research papers. He is there to help along every step of the way and always makes sure that his students leave with a proper understanding of the topic. Dr. Mulford was my professor for General Chemistry and my supervisor during my times as a TA for Organic Chemistry Lab. A part of my research involves polymer polymerization, which is something I first learned in Organic Chemistry Lab. Dr. Mulford gave me the opportunity to test out and ameliorate future experiments that will be used in future labs. Dr. Mulford's enthusiasm for chemistry has made a strong impression on me and I have always carried positive memories of his class.

Table of Contents

Introduction

Solid-Liquid Duality.....	1
Applications of Hydrogels.....	2
Non-Classical Friction.....	3
Frictional Transition Regimes in Hydrogel Systems.....	4
Hertzian Contact of Elastic Hydrogel systems.....	10

Materials and Methods

Types of Hydrogels.....	12
Ultra-Low Friction Tribometer.....	15
Determining Contact Area	15

Results and Discussions

Friction Coefficient vs Load.....	17
Changing Pore Size.....	19
Determining Contact Area under Varying Load.....	21
Determining Pore Size and Elastic Modulus.....	22

Final Remarks

Conclusion.....	25
Future Directions.....	25
References	26

List of Figures

Figure 1. Schematic Expansion of Gels.....	1
Figure 2. Friction Graphs with respect to Load and Velocity.....	3
Figure 3. Schematic of Gel-PMMA contact.....	4
Figure 4. Friction Coefficient vs Sliding Velocity for PAAm and Agarose	5
Figure 5. Schematic of a Fluid's Velocity Gradient.....	6
Figure 6. Schematic of a Velocity Gradient within Gel-PMMA Contact.....	8
Figure 7. Contact Stress of Hydrogel.....	10
Figure 8. Gelation of Agarose.....	13
Figure 9. Polymerization of Acrylamide and Bis-Acrylamide.....	14
Figure 10. Schematic of Tribometer.....	15
Figure 11. Contact Area Apparatus.....	16
Figure 12. Friction Coefficient vs Sliding Velocity for 2% Agarose.....	17
Figure 13. Friction Coefficient vs Variable Load.....	18
Figure 14. Agarose Gels of Variable Polymer Concentrations.....	19
Figure 15. Friction Coefficient vs Polymer Constitution.....	19
Figure 16. PAAm Gels Immersed in Variable NaCl Solutions.....	20
Figure 17. Friction Coefficient vs Variable NaCl Concentrations.....	20
Figure 18. Contact Area Images.....	21
Figure 19. Hertzian Contact Plot.....	21
Figure 20. Pore Size vs Gel Type.....	22
Figure 21. Elastic Modulus vs Gel Type.....	24

Introduction

Solid-Liquid Duality: Hydrogels are comprised almost entirely of water, yet we can hold onto them. Their state is neither completely liquid nor completely solid. They are slippery, like a fluid, yet rigid, like a solid. They deform with stress and recover their original shape after removing the stress, much like a solid would. They allow fluid convection and diffusion of solutes that are smaller than the mesh size of the network, much like a liquid would [1].

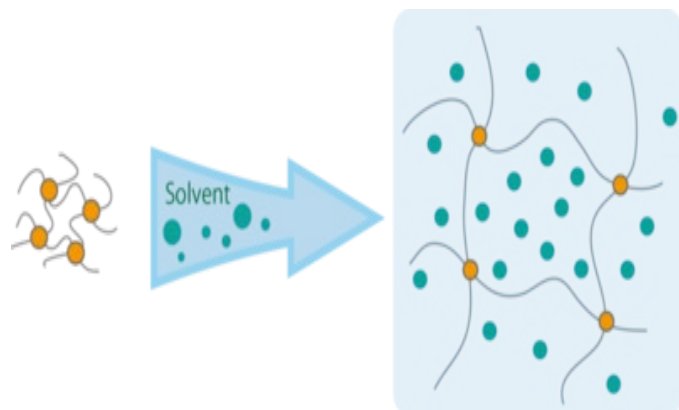


Figure 1: The schematic diagram of the network structure of gel, swelling when immersed into a solvent. The solid black lines denote polymer chains and the yellow circles denote cross-linking points. [2]

At a microscopic scale, hydrogels consist of long chain molecules (polymers) that are crosslinked to create a 3D polymer network capable of retaining large volumes of solvent. Their ability to absorb water arises from hydrophilic functional groups attached to the polymer backbone, which act as a matrix to attract and retain water molecules. As the liquid fills the pockets of empty space

in between the polymers, the network swells and expands out (Figure 1). These pockets can be defined as the largest sphere that encompasses the given point without overlapping the neighboring wall atoms [3]. The polymers, on the other hand, resist dissolution due to the crosslinks that exist between the polymer chains.

Common hydrogels such as polyacrylamide (PAAm) gels can absorb water up to 300 times the gel's own weight. They can vary in size, texture, and consistency from viscous fluids to fairly rigid solids based on interactions between the polymers and fluid and other external influences such as pH, pressure, light, ionization and more[4]. The dual identity of the hydrogel and its interactions with the environment make hydrogel mechanics a fascinating concept to investigate.

Applications of Hydrogels: Naturally, hydrogels' extensive properties make them a popular material of choice in various fields. Because the hydrogel can retain large volumes of water or other biological fluids, it is considered to have great potential for biomedical purposes. This concept makes them instrumental in the creation of bio-compatible devices such as contact lenses, hygiene products, and artificial tissues. Recently, hydrogels are attracting for their use in drug delivery because their stimuli-sensitive and adjustable porous structure allows selective drugs to be loaded and released through various controlled mechanisms [5]. Even in biology research, gels are used as an analytical tool, in which molecules are separated based on how quickly each sample can percolate through the pores of the gel [6]. They are widely used as a model in biology to mimic the physical, chemical and mechanical behaviors of the physiological environment. In the industrial and agricultural field, hydrogel's strong solvent absorption properties allow the invention of new artificial soils that boost the soil's capacity to hold water and diaper linings that absorb the moisture away from the baby's skin [4]. Because they are considered a recent development, there is an impetus to further our understanding of hydrogels' mechanical behavior.

Non-Classical Friction: Because of a hydrogel's soft and wet nature, another unique property arises: low friction. Our lab measured the frictional coefficient values as low as 0.001 on our ultra-low friction tribometer. Previous tribological studies investigated several factors that influence gel friction such as applied normal force [1], contact area [1], sliding velocity [7], and interfacial chemistry [8].

Gel friction is strange because it does not follow the classical friction model described by Amontons' laws. The laws state that frictional force is linearly proportional to normal load and does not depend on the sliding velocity and contact area between the surfaces [9]. However, studies have shown that the frictional coefficient is inversely related to normal load and frictional force changes non-monotonically with angular velocity in a rheometer (Figure 2) [1][10][11][12].

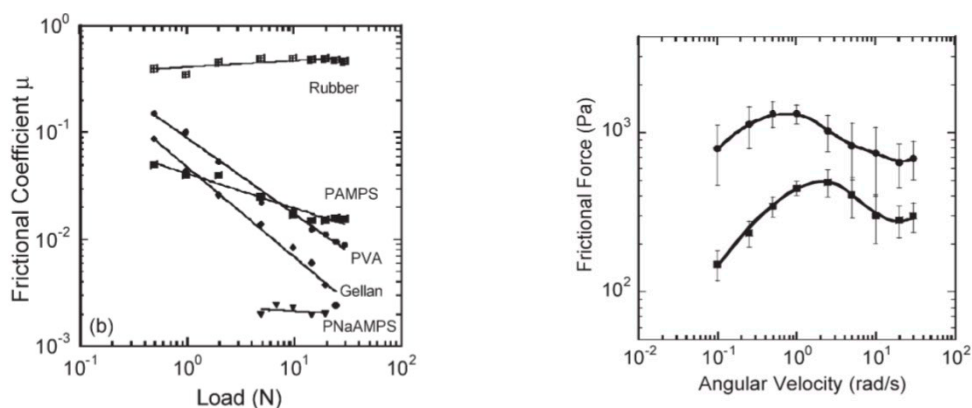


Figure 2: The left graph indicates coefficients of friction for different gels under varying load. The right graph indicates frictional force varying non-monotonically with increasing angular velocity [1].

Many models have been theorized to explain gel friction [13][14]. For example, Gong proposed a repulsion-adsorption model, which attributed frictional behavior from elastic deformation of polymer network due to gel adhesion to surface or from lubrication of polymer chains that are repulsive to the surface [13]. However, Gong's adsorption model was weakened by another study

which tested for hysteresis. Their results for PAAm-aluminum interfaces showed a significant hysteresis, which was not explained by Gong's adhesive model since it assumes symmetry in increasing and decreasing speeds [8]. With the increasing popularity of gel, a more robust model is still needed to understand the tribological model of gels.

Frictional Transition Regimes in Hydrogel Systems: Using our lab's ultra-low friction tribometer, we probed the single-contact frictional properties of spherical hydrogels on hard surfaces. In our experimental setup, we considered a lubricated contact between an elastic hydrogel body and a non-deformable surface at relative velocity. A load was applied such that there is substantial elastic deformation of the hydrogel (Figure 3). Because of the gel's solvated polymer network interacting with lubricated surfaces, we turned to a combination of hydrodynamic and polymer-surface interactions to explain gel friction.

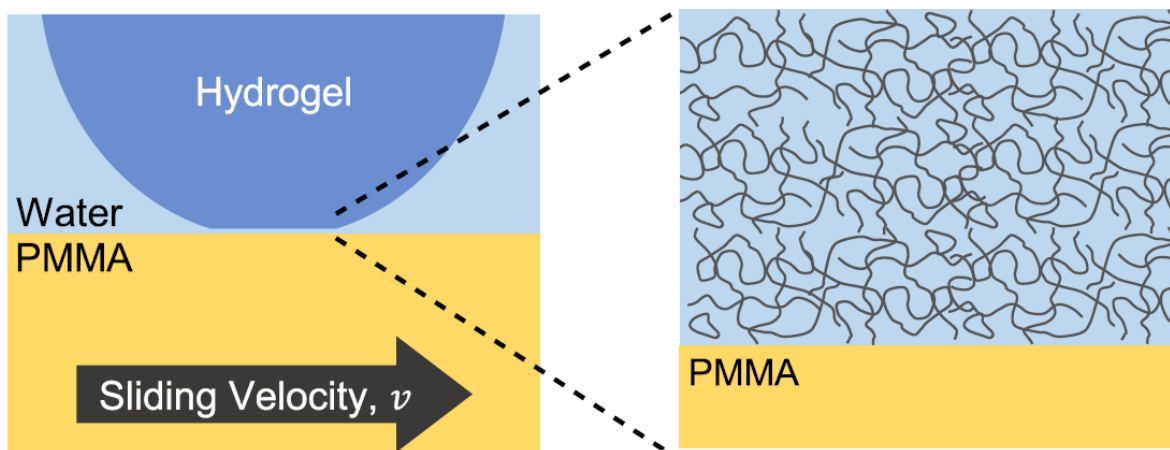


Figure 3: Experimental model set-up of spherical hydrogel in contact with a spinning acrylic (PMMA) disc. The black curves denote polymer strands that comprise of the hydrogel.

Our experimental results presented interesting frictional phenomena that occur when the coefficient of friction (μ) between the hydrogel and PMMA is measured at varying sliding

velocities (v) (Figure 4). Below I will describe these frictional phenomena by dividing them into three distinct regimes. The goal of this paper is to deduce equations of the frictional coefficient, mainly in the first regime, expressed as functions of experimental parameters such as the load, sliding velocity, contact area and fluid viscosity. Investigating this proposed model may help gain insight into subsequent regimes.

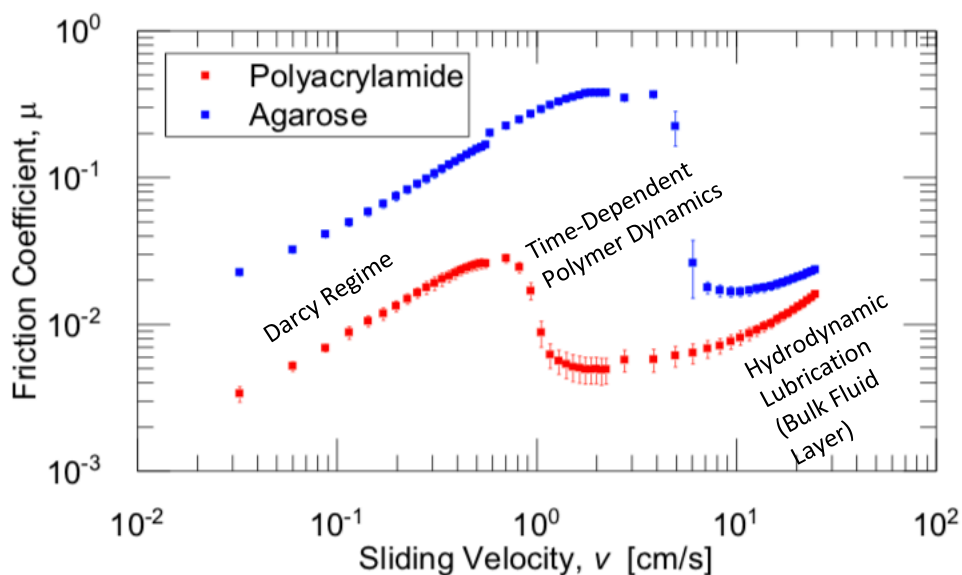


Figure 4: Friction coefficient (μ) of 29:1 PAAm and 2% Agarose hydrogels on PMMA under a constant normal force of 0.2N and varying sliding velocity.

In the Darcy regime, where there is gel-surface contact, we observed a linear increase in friction coefficient with respect to increasing sliding velocity. This behavior existed at low velocities. We predicted that this regime is influenced by viscous stresses because the hydrogel, which is almost entirely composed of fluid, undergoes shear stress as the PMMA surface spins with a sliding velocity. This can be visualized by a parallel-plate model, in which one plate is fixed and one is moving with a constant speed, u , that is low enough to not cause turbulence of fluid that exists

between the two regions. Going from the bottom plate to the top plate, the speed should vary from 0 to u , with each layer of fluid moving faster than the one below (Figure 5).

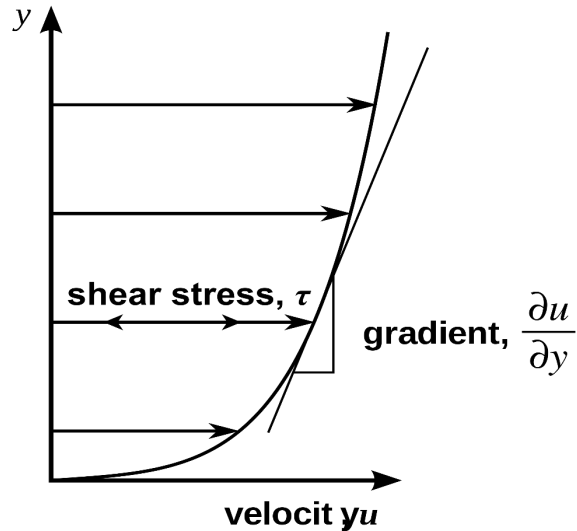


Figure 5: Velocity at the bottom is zero and rises to a velocity, u , at the top. Each layer of fluid moves faster than the one just below it. The velocity gradient is proportional to the shear stress of the fluid. Our derivation below replaces the variable u with v , which indicates the sliding velocity of the PMMA surface. [15]

Our goal is to determine an equation which defines the friction coefficient. First, we define shear stress (τ) as a ratio of the horizontal force applied to the hydrogel surface (F_{shear}) and the hydrogel's contact area (A). This is shown in the equation below.

$$\tau = \frac{F_{\text{shear}}}{A} \quad (1)$$

Then we define shear rate (γ) as the ratio of the relative sliding velocity (v) of the hydrogel surface and the thickness of the fluid film (h). This is shown in the equation below.

$$\gamma = \frac{v}{h} \quad (2)$$

Finally, we can define Newton's law of viscosity by dividing Eq. 1 and Eq. 2. This ratio yields the viscosity of the fluid film, as shown in the equation below.

$$\eta = \frac{F_{\text{shear}} \cdot h}{A \cdot v} \quad (3)$$

By rearranging and solving for the shear force, we get

$$F_{\text{shear}} = A \eta \frac{v}{h} \quad (4)$$

We can then determine the friction coefficient by dividing Eq. 4 by the applied load (N), which is shown below.

$$\mu = \frac{F_{\text{shear}}}{N} = \frac{A \eta v}{N h} \quad (5)$$

According to Fig.4, agarose exhibited a higher friction coefficient compared to the PAAm. One of the main differences between the two gels possibly attributing to the increased friction coefficients was their pore size. To describe the phenomenon, we assumed that the lubrication layer thickness is proportional to the characteristic pore size of the hydrogel, d . In a recent study by Carotenuto and Minale, a velocity profile between a hard surface and a porous medium was developed to characterize shear flow. In the shear-driven case, the velocity gradient, or also known as shear rate, is supposed to be approach zero as it nears the stationary surface. Instead, the velocity was nonzero at the surface and seen decaying into the porous medium's transition layer. The flow into the transition layer zone was inherently a surface phenomenon strongly affected by the interface topology of the porous medium [16]. We considered the length of the transition layer into which the fluid flows through to be proportional to the pore size of the hydrogel of interest, which we defined as d , the characteristic pore size (Figure 6).

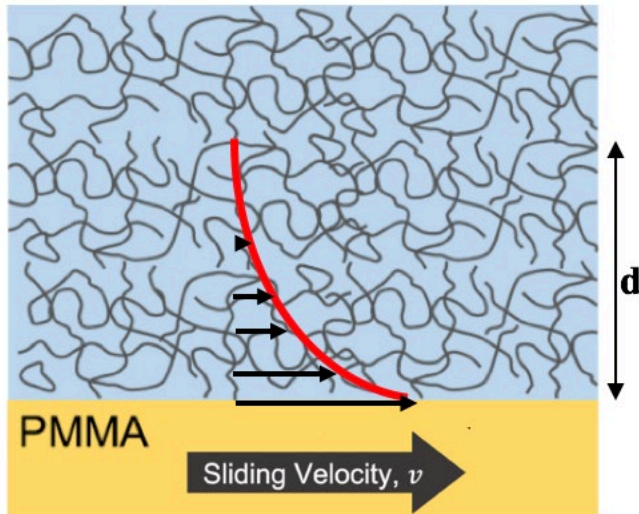


Figure 6: Velocity profile of fluid over and into porous medium for a shear-driven flow. The length of transition layer in which the velocity is seen to decay into is assumed to be proportional to the hydrogel's pore size (d).

With this assumption, we can now replace the variable h with d in Eq. 5 to get Eq. 6.

$$\mu = \frac{A\eta v}{N d} \quad (6)$$

This regime was called the Darcy regime due to our assumption that fluid flows through the porous medium to a length scale proportional to pore size. In our investigation, we altered the pore size of the hydrogels to see how friction coefficient changes and obtained experimental pore sizes from our proposed model to compare them with already known values of hydrogel pore sizes.

The end of the Darcy regime was indicated by a stark decrease in frictional coefficients at a critical sliding velocity (v_c). With speeds faster than v_c , we observed that the friction coefficient was time-dependent, with a characteristic decay time of order 10 minutes. An increase in sliding velocity

causes more fluid to move into the space in between the surfaces. Significant in this regime, upward forces from the fluid pushes the surfaces apart, causing the friction to lower.

A property that we observed in this regime was that upon inverting the system from a gel ball on PMMA disc to that of PMMA ball on a gel disc, this frictional phenomenon disappeared. What was more interesting was that when the stress caused by shear-driven flow was removed briefly, the friction had a rapid recovery rate. Our results can be interpreted as a competition between the shear rate in the fluid versus the relaxation time it takes the polymer chains to return to equilibrium after being disturbed. In the case of the gel ball on PMMA disc, the same point of contact of the gel was being sheared continuously for a long time and being subjected to great stress. However, in the PMMA ball on gel disc, new parts of the gel were being sheared such that its stress was minimal. Therefore, we saw significant stress relaxation behavior in the case of gel ball on PMMA disc. This non-monotonic frictional behavior was robust, occurring across both chemical and physical hydrogels of differing molecular compositions.

When under such strain, the stress in the gel relaxes by different mechanisms, depending on the crosslinking. Physical gels, which are governed by non-covalent bonds, relax by breaking and reforming these bonds, resulting in an elastic deformation. Chemical gels, which are governed by covalent bonds, relax through water efflux [17]. We witnessed this when, at the end of our tribometer trials, our agarose hydrogels were deformed into a flat plane towards the bottom while the polyacrylamide hydrogels were able to retain their original shape.

Finally, as we increased sliding velocity even more, we transitioned from the Time-dependent polymer dynamic regime to the Hydrodynamic Lubrication regime. At very high velocities, the gel-surface contact is separated by a lubricant film due to an increase in hydrodynamic pressure. At the lowest point of the curve shown in Fig.4, the gel and PMMA surfaces were barely touching. However, once the hydrodynamic pressure increases, the fluid film in between gets thicker and the internal friction increases [18][19].

Hertzian Contact of Elastic Hydrogel Systems: As seen in Eq. 6, determination of contact area is crucial for determining pore size. We considered a loaded, lubricated contact between an elastic spherical hydrogel and a non-deformable surface at relative velocity. The normal load must be large enough to cause an elastic deformation that is nearly flat to be considered a Hertzian geometry contact. Assuming the hydrogel to be a sphere of radius R that is subject to a load N , the downward force causes the sphere to indent into the elastic half-space to depth z and create a contact area of radius a (Figure 7).

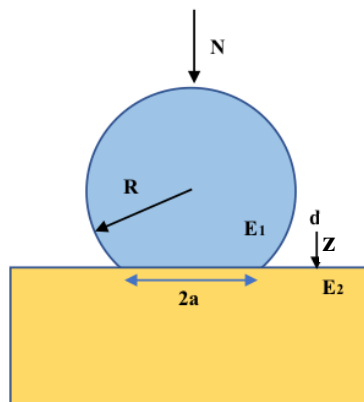


Figure 7: Contact stress of hydrogel. The blue circle is the hydrogel with an elastic modulus E_1 , sphere radius R and contact radius a . The yellow rectangle is an elastic half-space with elastic modulus E_2 . Depth z is how much the elastic half-space indents from the hydrogel and load. With increasing loads, the gel widens horizontally to preserve volume changes.

The contact radius can be defined by the equation

$$a = \sqrt{Rz} \quad (7)$$

The load N can be written in terms of depth z as

$$N = \frac{4}{3} E^* R^{1/2} z^{3/2} \quad (8)$$

Where

$$\frac{1}{E^*} = \frac{1-\nu_1^2}{E_1} + \frac{1-\nu_2^2}{E_2} \quad (9)$$

E_1, E_2 are Young's moduli for the gel and PMMA while ν_1, ν_2 are Poisson's ratios for the gel and PMMA, respectively. We can solve for the contact radius a by combining Eq. 7 and Eq. 8 to get the equation below [20].

$$a^3 = \frac{3NR}{4 E^*} \quad (10)$$

The Hertzian contact theory also lets us determine the elastic modulus of the gel, which is essentially a ratio between stress and strain. A hydrogel with high concentration of cross-linking results in a stiffer material and so will have a higher elastic modulus. The elastic modulus is an important property that may help in understanding the time-dependent polymer dynamics regime. As strain is increased in gels, not only do gels stiffen but they also exhibit faster stress relaxation, reducing the timescale over which elastic energy is dissipated, suggesting a possible correlation between stress relaxation behavior and elasticity [21].

Looking back at Eq. 9, we can assume the 2nd term is negligible because PMMA's elastic modulus is around 3 GPa. Then Eq. 9 can be rewritten as

$$E_1 = E^*(1 - \nu_1^2) \quad (11)$$

As mentioned before, studies showed an inverse relation between load and frictional coefficient.

We can plug in Eq. 10 into Eq. 6, in which A is equal to πa^2 , and get the equation below.

$$\mu = \pi \left(\frac{3R}{4E^*} \right)^{\frac{2}{3}} \left(\eta \frac{v}{d} \right) (N)^{-\frac{1}{3}} \quad (12)$$

The equation above indicates that if we increased the load on the gel, we should expect decreases in friction coefficients by a small factor.

Materials and Methods

Types of Hydrogels: While hydrogels can be classified into various categories based on their different properties, our study focused on the mechanism of polymer cross-linking, which can be divided into physical cross-linking and chemical cross-linking. Our study used self-manufactured agarose and PAAm hydrogels.

Agarose hydrogels are physical gels because the agarose chains, upon cooling, form helical fiber bundles held together by hydrogen bonds (Figure 8). The interaction among the helices causes gelation. These hydrogen bonds can be thermally reversed by heating the gel back into the liquid state. Generally, agarose hydrogels were prepared using a w/v percentage solution by mixing the appropriate mass of agarose into a 1xTAE buffer solution. Within the experiment, gels with agarose percentages 0.5%, 1%, 1.5%, 2% were made. The gels were cast in a spherical silicone mold of roughly 4mm in diameter.

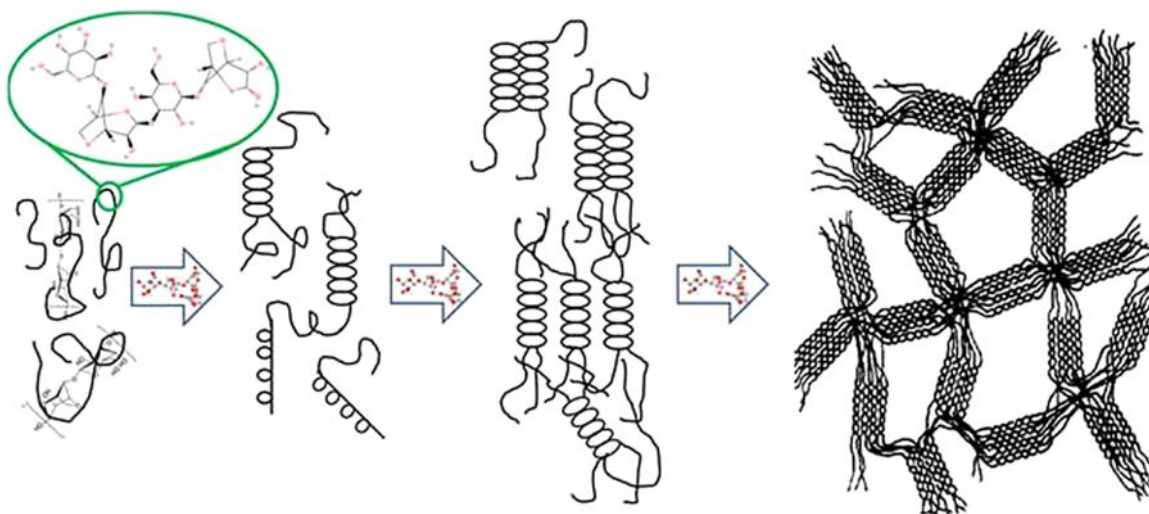


Figure 8: Gelation of agarose. Agarose chains tend to form hydrogen bonds and electrostatic interactions that lead to helical structures. [22]

Polyacrylamide hydrogels are chemical gels because the polymers undergo irreversible covalent crosslinking via free-radical polymerization. Initially, we prepared a solution of acrylamide and bis-acrylamide (N,N' -methylenebisacrylamide) monomers. Ammonium persulfate (APS) was added to act as a source of free-radicals that convert acrylamide monomers to free radicals which in turn reacted with other monomers to begin a polymerization chain reaction. The elongating polymer chains were randomly crosslinked by bis-acrylamide, resulting in a gel with a characteristic porosity that depends on monomer concentrations. TEMED (tetramethylethylenediamine) was also added to increase the rate of free-radical formation from APS and in turn catalyze polymerization (Figure 9).

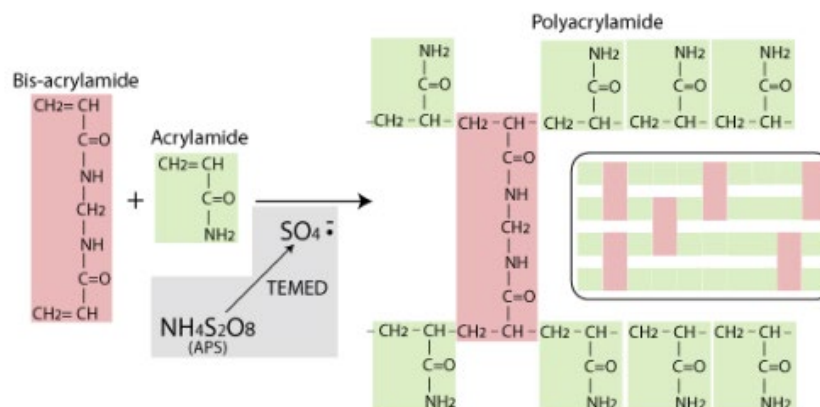


Figure 9: Polymerization between acrylamide (a monomer) and bis-acrylamide (a crosslinking monomer). TEMED turns APS into a free radical that enables polymerization [23].

Polyacrylamide gels are characterized by %T and %C. The total monomer concentration (%T) is given by the ratio of total mass of acrylamide and cross-linker and total volume of the solution. The weight percentage of crosslinker (%C) is given by the ratio of mass of cross-linker to total mass of acrylamide and cross-linker. With increasing %T, we should expect to see smaller pores because the density of the polymers was increasing. Pore size and %C also indicated a negative correlation from 1% to 5%. This was because as we increased the amount of cross-linking, more bonds between acrylamide monomers were created. Any %C values greater than 5 would have pore size values similar to pore sizes associated %5 [24]. This observation may be explained by acrylamide monomers cross-linking sites to have been saturated with cross-linkers and the free crosslinkers were either resting within the pore sizes or migrating out of the porous structure. Within the experiment, gels with ratios of 9:1, 19:1, 29:1 acrylamide to bis-acrylamide were made. All PAAm gels made have a %T=8. The gels were cast in the same molds used for agarose hydrogels.

Ultra-Low Friction Tribometer: To determine friction coefficients, we used a custom pin-on-disc tribometer (Figure 10). We varied the speed at which the PMMA disc spun by attaching voltage variable DC motors. We used three different DC motors (low, medium and high-velocity) to precisely control the sliding velocity of the acrylic disc (0.01cm/s to 20cm/s). On the edge of the disc was a S256 10g Force Sensor from Strain Measurement Devices that has a force sensor resolution of down to 0.2 mN so that we can measure small force fluctuations. The force sensor was connected to our computer by wiring it through an NI USB-6525 data acquisition device (DAQ) from National Instruments. Data was collected through the LabView software which controlled and managed the DAQ. Load can be applied to the system by adding masses to the top of the force sensor.

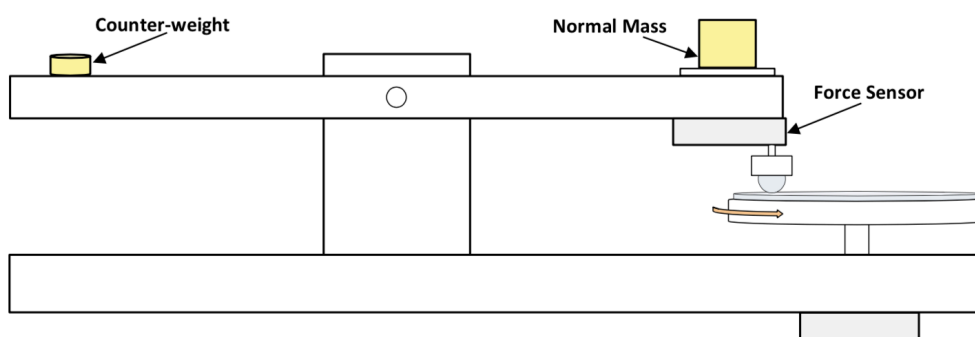


Figure 10: Schematic of a pin-on-disc tribometer, designed by Nicholas Cuccia.

Contact Area Apparatus: To determine the contact area, we devised an optical set-up that imaged the surface of a hydrogel under varying load. We suspended a hydrogel in an open acrylic cube filled with water and red, fluorescent, polyethylene microspheres. On top of the hydrogel, we placed a stand that secures the hydrogel into the center of the cube. The stand rested on top of the gel such that we could place masses on top in a controlled manner to apply load. We varied the masses from 0g to 40g with increments of 2.5g. Under a load, the hydrogel surface will be

compressed, and the outer part of the surface will be surrounded by the microspheres. We chose $\sim 63\text{-}75\mu\text{m}$ wide microspheres because the size is substantial enough that they are not subjected to Brownian motion and they will have settled on the bottom after a few minutes passed. The particles were also small such that they can fit into the crevices near the hydrogel's surface. Green fluorescent light was placed at the bottom to illuminate the microspheres (Figure 11). A camera was directed towards a half-mirror, which is placed at an angle to reflect the hydrogel's surface.

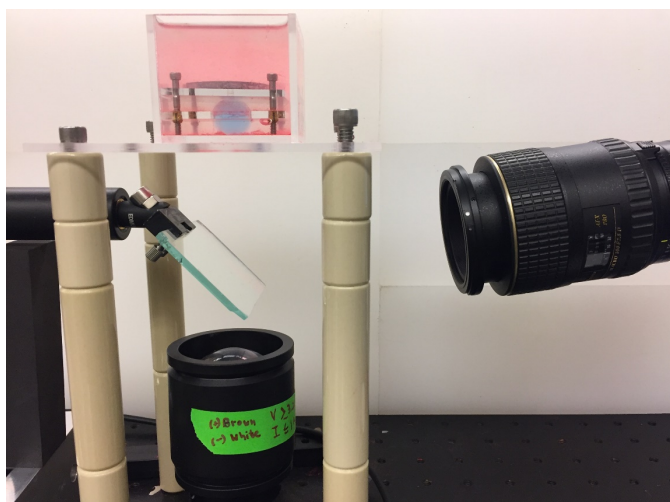


Figure 11: Contact Area Apparatus. A camera faces an angled half-mirror that reflects the bottom of the hydrogel. A PAAM hydrogel is placed within an acrylic box filled with red fluorescent microspheres.

Results and Discussion

Friction Coefficient vs Load: The main goal of this investigation was to determine if there was a pore size dependence on friction coefficient within the Darcy regime. Before we tested this relationship, we began with a verification to check if our set-up gives us already predicted values. First, we applied a load of 0.1N to a 2% agarose gel and measured the friction coefficient under variable sliding velocities. All plots were put into a log-log scale format. Fig. 12 below shows that our measurements did not have significant variation across several trials and that friction coefficients were below 0.2, indicating low friction typical for gels. Another interesting observation from our experiments was that $\mu \sim v^\beta$, in which $\beta = 1$. However, β can range from 0.5 to 1, which indicated that hydrostatic friction plays a role.

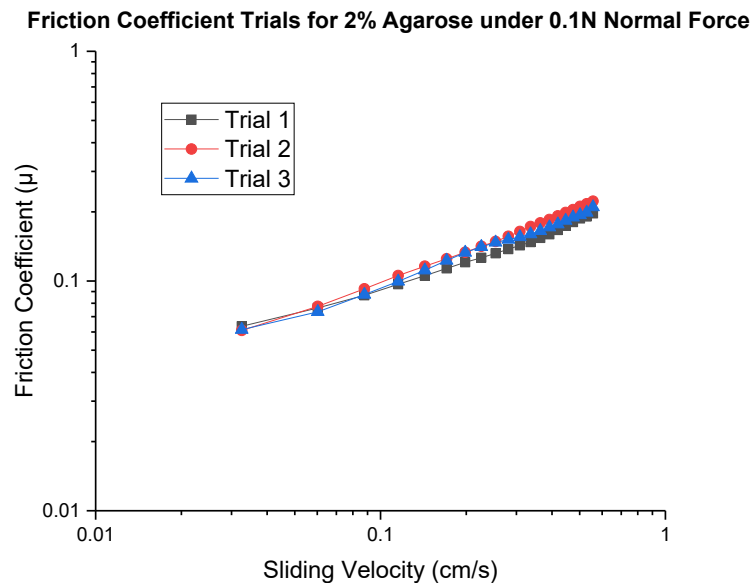


Figure 12: Measurement of friction coefficient under variable sliding velocities for agarose gel on PMMA disc. Three trials were done with different 2% agarose gels with a load of 0.1N.

Next, we tested to see if we can get an inverse relationship between friction coefficient and load, as indicated by Eq. 12. Using the same range of sliding velocities from Fig.12, we tested 2% agarose and 29:1 PAAm and varied the load by using 10g, 20g and 40g masses. As indicated in Fig.13, both agarose and PAAm decreased in friction coefficient values as we increased the load. For instance, in the agarose graph, when we increased the load by a factor of 4, friction coefficient decreased only by a factor of 1.6. The small factor of decrease agreed with Eq. 12 which states that friction coefficient cubed negatively correlates with load. The 29:1 PAAm gel exhibited friction coefficient values much lower than 2% agarose, which could possibly be explained by the 2% agarose having a smaller pore size due to the high density of polymers. As shown by Eq. 6, friction coefficient has an inverse relationship with pore size, d and thus, 2% agarose gel's small pore size could have led to friction coefficients much higher than those of PAAm.

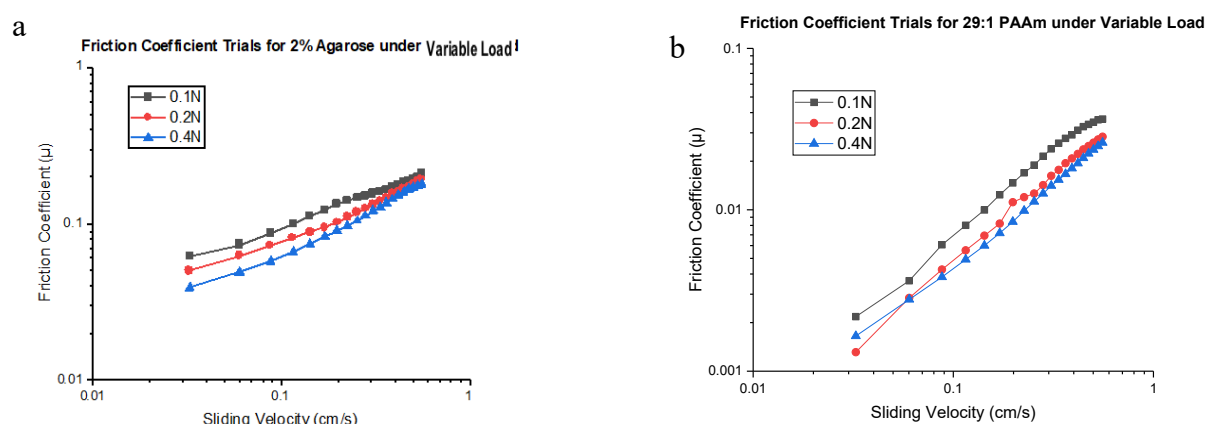


Figure 13: Measurement of friction coefficient under variable load for a) 2% Agarose and b) 29:1 PAAm gel on PMMA disc. The masses used were 10g, 20g, and 40g.

Changing Pore Size: Now that we proved an inverse relation between load and friction coefficient, we moved onto the main investigation. To test for pore-size dependence, we varied the pore size of agarose by altering the agarose concentration because an increase in polymer density concentration should result in a



Figure 14: Agarose gels of different concentrations. From left to right, the agarose gels start with 0.5%, 1%, 1.5% and 2%.

decrease in average pore size within the gel. Agarose gels with concentrations 0.5%, 1%, 1.5% and 2% were tested under 0.1N of load (Figure 14). We varied the pore size of PAAm by changing %C. Based on studies by Stellwagen, 29:1 gels had a pore size of 100-120 nm, while both 19:1 and 9:1 have a pore size of 20-40 nm [24]. Based on Eq. 6, there should be an inverse relationship between pore size and friction coefficient. As shown in Fig.15 below, an increase in agarose concentration, which leads to a decrease in pore size, positively correlated with an increase in friction coefficient values. In PAAm gels, we observed that the 19:1 and 9:1 friction coefficients were similar while the 29:1 friction coefficients were much lower.

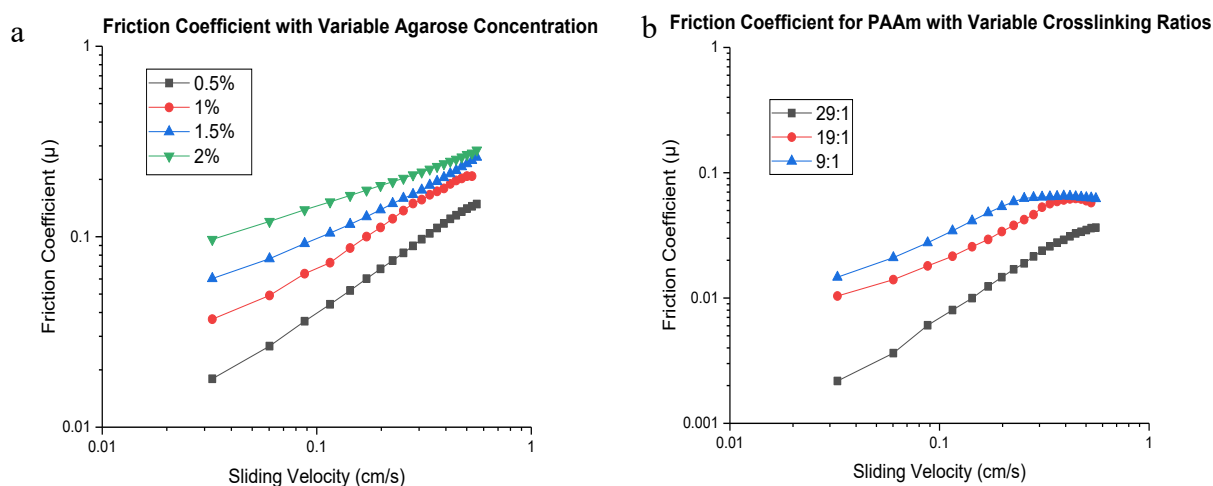


Figure 15: Measurement of friction coefficient under a) variable agarose concentration and b) variable crosslinking ratios. The load was kept consistent at 0.1N.

Next, we changed the pore size for both agarose and PAAm gels by varying the NaCl salt concentrations in which each hydrogel was immersed in. We placed the gels in 0.001M, 0.01M and 0.1M salt solutions such that water within the hydrogels will migrate out and into the hypertonic solution. As the hydrogel shrinks, the pore size should shrink too. The agarose gels' radii decreased very slightly while the 29:1 PAAm gels' radii decreased significantly (Figure 16).

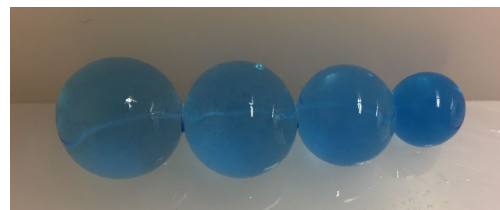


Figure 16: 29:1 PAAm subject to different saline conditions (NaCl). From left to right, the PAAm gels start with 0M, 0.001M, 0.01M and 0.1M.

When the hydrogels were subject to increasing salt concentrations, which should lead to a decrease in pore size, both gels' friction coefficients increased (Figure 17). These results showed that varying the pore size does indeed have an effect on friction for both agarose and PAAm gels. However, to see if the effect is directly related to pore size, we must account for the contact area that each gel exhibits under varying load.

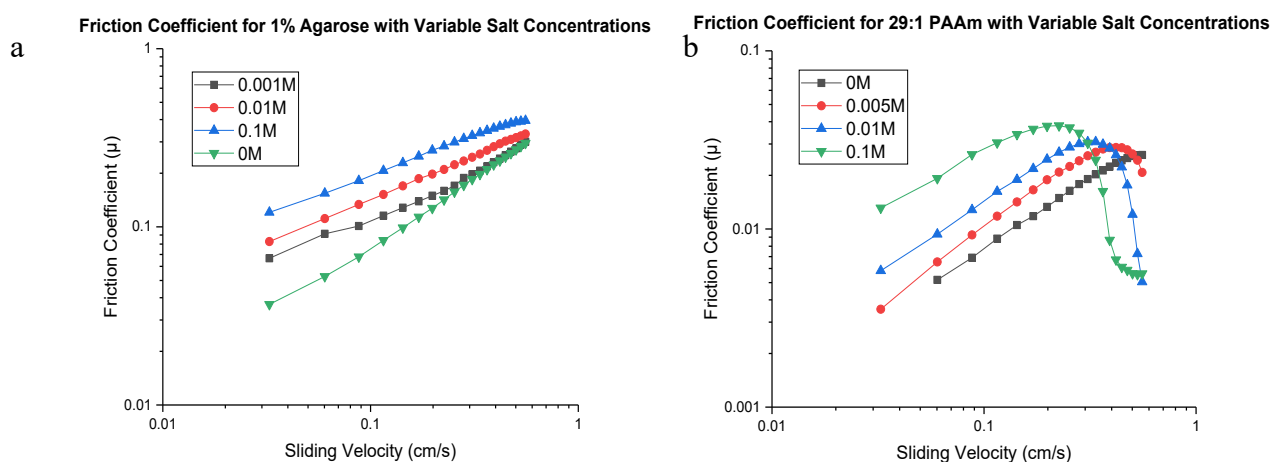


Figure 17: Measurement of friction coefficient of a) 1% agarose gel under variable salt concentrations and b) 29:1 PAAm gel under variable salt concentrations. The load was kept consistent at 0.1N. The PAAm curves in the right graph that begin to curve downwards towards the later range of velocities indicate a transition into the next regime.

Determining Contact Area under Varying Load: To measure the contact area for each gel for varying loads, we used the contact area apparatus (Figure 18). Using Eq. 10, we plotted the load N as a function of contact radius cubed a^3 with a trend line of slope $(\frac{3NR}{4E^*})$ to see if our hydrogels exhibit Hertzian geometry. Our plots showed a strong linear dependence between load applied to hydrogel and its contact radius cubed, which indicated that the hydrogels are experiencing Hertzian geometry (Figure 19).

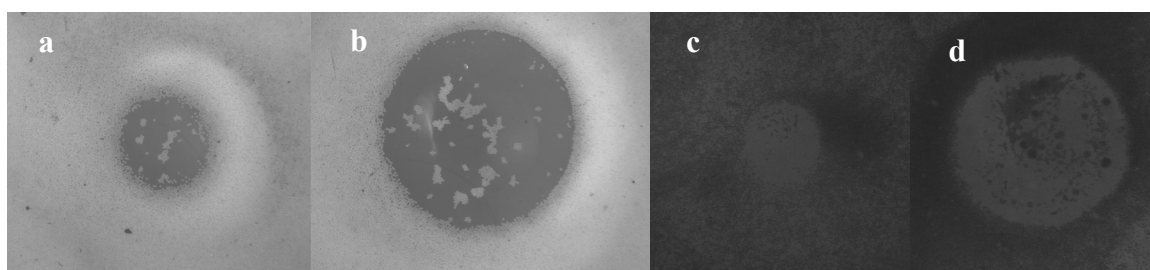


Figure 18: Measurement of Contact radius for a) 29:1 PAAm under 13.6mN load, b) 29:1 PAAm under 355mN load, c) 1% agarose under 16.7mN load, and d) 1% agarose under 188mN load

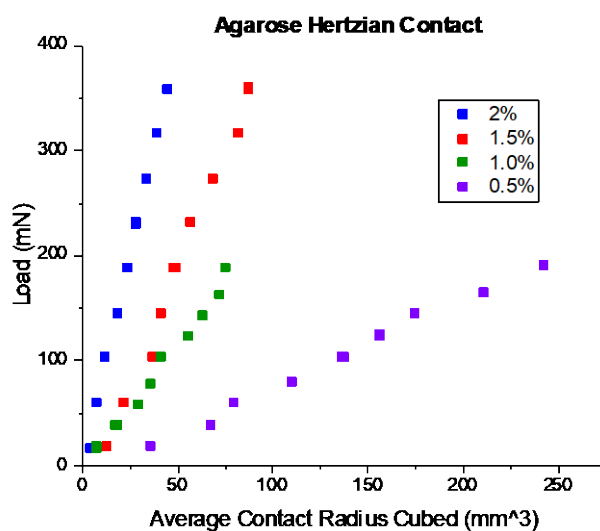


Figure 19: Hertzian contact plot for 1% agarose gel. Load (N) is plotted as a function of average radius cubed.

Based on the plots for each gel, we inputted the load used in the friction experiments into the linear trend line equations to solve for a^3 and in turn, the contact area of the hydrogel. A limitation in this experimental set up is the particle size of the fluorescent microspheres. Though the microspheres chosen are small, varying from 63-75 microns, their size might still be too large to fit into the crevices of the hydrogel at the bottom. This will result in a larger than expected contact radius.

Determining Pore Size and Elastic Modulus: Now that we measured the contact radius for all our gels under any load and accounted for all other variables from Eq. 6, we determined the characteristic pore size d for each gel type that was experimented with. Although our experimental characteristic pore size values should collapse to a point, we observed a relatively small range of values (Figure 20). Considering the contact area limitation mentioned before, our experimental pore sizes will be slightly larger than expected.

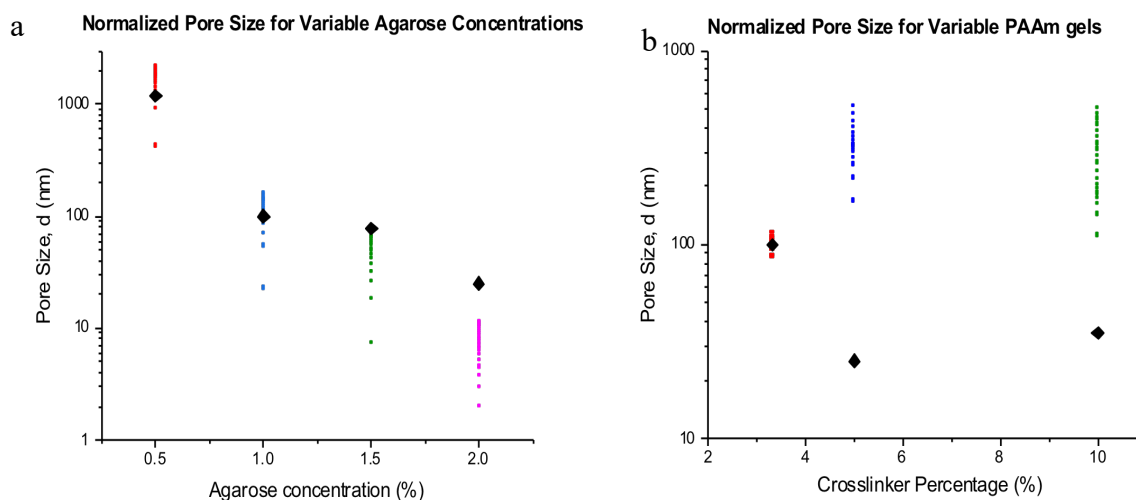


Figure 20: Pore Size values for a) variable agarose concentrations and b) variable acrylamide to bis-acrylamide ratios. The diamond points represent pore size values from various literatures. [24][25][26]

As we increased agarose concentration, we saw a decrease in pore size values, which agrees with our Eq. 6. Furthermore, we noticed that our characteristic values are in very close proximity to literature values. If we were to define our characteristic pore size, d , as $d = Cd^*$, in which C is the proportionality constant and d^* is the actual pore size, then C is approximately equal to 1. This case followed for 29:1 PAAm gel also. However, for 19:1 and 9:1 PAAm gels, the C was close to a factor of 10. A possible explanation for such a difference might be because with increasing cross-linker, the acrylamide monomers are already fully saturated with cross-linker and extra cross-linker settles in between the pores. Furthermore, the crosslinking process might not be heterogeneous because when we observed 9:1 PAAm gels swelling, we noticed that swelling took place in certain areas before others. These phenomena may have played a role in producing pore sizes that are similar to pore sizes found in 29:1.

Hydrogel pore size determination research is yet to be established and the ones that are available show large variations in values depending on their methodology. For instance, agarose gel pore radius is estimated to be around 100nm for 1% agarose based on electrophoretic studies. However, Ferguson plot analysis tend to lead to values that are ~2-fold larger than those determined by electrophoretic methods, while the gel pore radii measured by NMR or atomic force microscopy (AFM) are ~2-fold larger compared to the electrophoretic methods [25].

Next, we measured the elastic moduli (E) for each gel using Eq. 11 and the E^* values obtained from the trendline slopes of the previous section. As shown in Fig.21 below, Poisson ratios of 0.5 were calculated to create a range of values for elastic moduli. The gel got stiffer as agarose concentration increased and PAAm cross linker concentration decreased. Literature values

indicated that the elastic moduli of 0.5%, 1% and 2% agarose were determined to be around 2 kPa, 17 kPa, and 55 kPa, respectively, assuming a Poisson ratio of 0.5 [26].

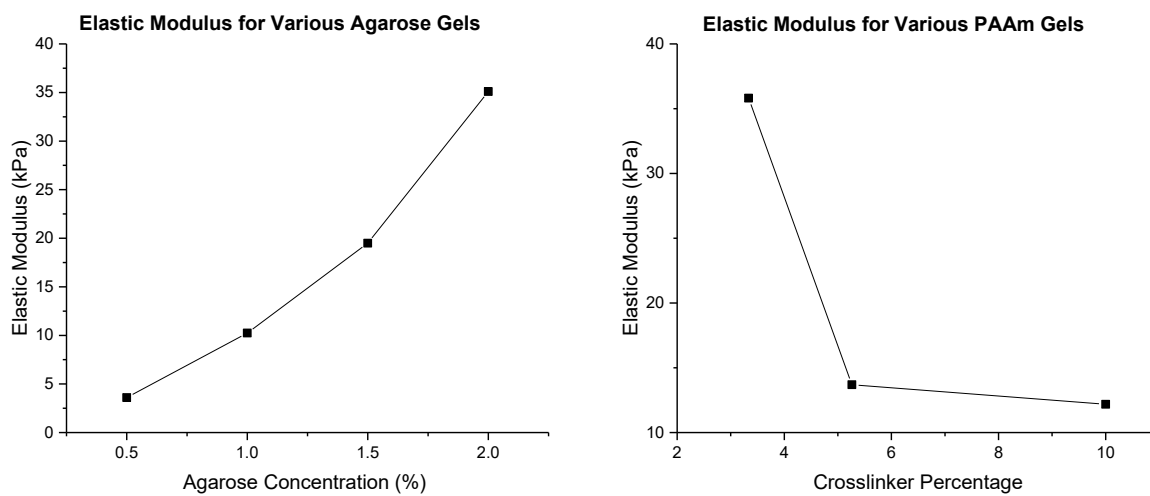


Figure 21: Elastic moduli for a) variable agarose concentrations and b) PAAm gels with variable acrylamide to bis-acrylamide ratios.

Final Remarks

Conclusion: The goal of this experiment was to test our model for the Darcy regime of the gel friction curve, determine a pore size dependence on friction coefficient for both physical and chemical gels, determine exact values of pore size and elastic moduli. Using our custom tribometer, we were able to establish that both physics and chemical gels behave similarly at low-velocity regimes. From our measurements, we have shown a positive correlation between friction coefficient and sliding velocity and have shown a negative correlation between friction coefficient and load. We varied the pore size of both agarose and PAAm gels through changing agarose concentration and crosslinker concentration, respectively, and have shown a negative correlation between friction coefficient and pore size. We measured the contact area of each gel tested to determine exact pore size values and elastic moduli. The agarose gels agreed with our theoretical predictions but the PAAm gels did not. A possible explanation for such a difference might be because of over-saturated cross-linking binding sites on these gels, non-uniform swelling and large surface asperities that cause an increase in friction.

Future Directions: We wish to investigate PAAm gels more in the future and establish a reason for its behavior. Instead of changing %C, we will change %T and expect a similar trend as agarose gels. Furthermore, we wish to investigate the time-dependent polymer extension regime by creating an optical set-up at the hydrogel's surface to see if polymer dynamics is responsible for the stress relaxation behavior.

References

- 1 Gong, J. P. (2006). Friction and lubrication of hydrogels—its richness and complexity. *Soft matter*, 2(7), 544-552.
- 2 Imran, A. B., & Takeoka, Y. (2015, April 02). The development of novel "stimuli-sensitive" hydrogels for various applications | Highlights. Retrieved from http://www.aip.nagoya-u.ac.jp/en/public/nu_research/highlights/detail/0001878.html
- 3 Bhattacharya, S., & Gubbins, K. E. (2006). Fast method for computing pore size distributions of model materials. *Langmuir*, 22(18), 7726-7731.
- 4 Ahmed, E. M. (2015). Hydrogel: Preparation, characterization, and applications: A review. *Journal of advanced research*, 6(2), 105-121.
- 5 Chai, Q., Jiao, Y., & Yu, X. (2017). Hydrogels for biomedical applications: their characteristics and the mechanisms behind them. *Gels*, 3(1), 6.
- 6 Tanaka, T. (1981). Gels. *Scientific American*, 244(1), 124-S.
- 7 Kagata, G., Gong, J. P., & Osada, Y. (2002). Friction of gels. 6. Effects of sliding velocity and viscoelastic responses of the network. *The Journal of Physical Chemistry B*, 106(18), 4596-4601.
- 8 Kim, J., & Dunn, A. C. (2016). Soft hydrated sliding interfaces as complex fluids. *Soft matter*, 12(31), 6536-6546.
- 9 Introduction to Tribology – Friction. (n.d.). Retrieved from <http://depts.washington.edu/nanolab/ChemE554/Summaries ChemE 554/Introduction Tribology.htm>
- 10 Gong, J. P., Iwasaki, Y., & Osada, Y. (2000). Friction of gels. 5. Negative load dependence of polysaccharide gels. *The Journal of Physical Chemistry B*, 104(15), 3423-3428.
- 11 Yoshida, K., Yahagi, H., Wada, M., Kameyama, T., Kawakami, M., Furukawa, H., & Adachi, K. (2018). Enormously Low Frictional Surface on Tough Hydrogels Simply Created by Laser-Cutting Process. *Technologies*, 6(3), 82.
- 12 Urueña, J. M., McGhee, E. O., Angelini, T. E., Dowson, D., Sawyer, W. G., & Pitenis, A. A. (2018). Normal load scaling of friction in gemini hydrogels. *Biotribology*, 13, 30-35.
13. Gong, J., & Osada, Y. (1998). Gel friction: a model based on surface repulsion and adsorption. *The Journal of chemical physics*, 109(18), 8062-8068

- 14 Pandey, A., Karpitschka, S., Venner, C. H., & Snoeijer, J. H. (2016). Lubrication of soft viscoelastic solids. *Journal of fluid mechanics*, 799, 433-447.
- 15 “Viscosity.” Wikipedia, Wikimedia Foundation, 6 Apr. 2019, en.wikipedia.org/wiki/Viscosity.
- 16 Carotenuto, C., & Minale, M. (2011). Shear flow over a porous layer: Velocity in the real proximity of the interface via rheological tests. *Physics of Fluids*, 23(6), 063101.
- 17 Zhao, X., Huebsch, N., Mooney, D. J., & Suo, Z. (2010). Stress-relaxation behavior in gels with ionic and covalent crosslinks. *Journal of applied physics*, 107(6), 063509.
- 18 “Stribeck Curve.” Grundfos, 24 Aug. 2017, www.grundfos.com/service-support/encyclopedia-search/stribeck-curve.html.
- 19 “Tips and Tricks from Joe Flow – Stribeck Curves: A ...” World of Rheology, Anton Paar, www.world-of-rheology.com/fileadmin/public/rheology/Tips_Tricks_Joe_Flow?XRRIA021EN-A_Joe_Flow_Stribeck_Curves.pdf.
- 20 Contact mechanics. (2019, March 16). Retrieved from <http://en.wikipedia.org/wiki/Contactmechanics>
- 21 Nam, S., Hu, K. H., Butte, M. J., & Chaudhuri, O. (2016). Strain-enhanced stress relaxation impacts nonlinear elasticity in collagen gels. *Proceedings of the National Academy of Sciences*, 113(20), 5492-5497.
- 22 Zarrintaj, P., Bakhshandeh, B., Rezaeian, I., Heshmatian, B., & Ganjali, M. R. (2017). A novel electroactive agarose-aniline pentamer platform as a potential candidate for neural tissue engineering. *Scientific reports*, 7(1), 17187.
- 23 Agarose Gels Do Not Polymerise! (2008, August 06). Retrieved from <https://bitesizebio.com/10248/agarose-gels-do-not-polymerise/>
- 24 Stellwagen, N. C. (1998). Apparent pore size of polyacrylamide gels: Comparison of gels cast and run in Tris-acetate-EDTA and Tris-borate-EDTA buffers. *Electrophoresis*, 19(10), 1542-1547.
- 25 Stellwagen, N. C. (2009). Electrophoresis of DNA in agarose gels, polyacrylamide gels and in free solution. *Electrophoresis*, 30(S1), S188-S195
- 26 M.L. Oyen, “Mechanical Characterisation of Hydrogel Materials”, *International Materials, Reviews*, 59:1, 44-59, 2013